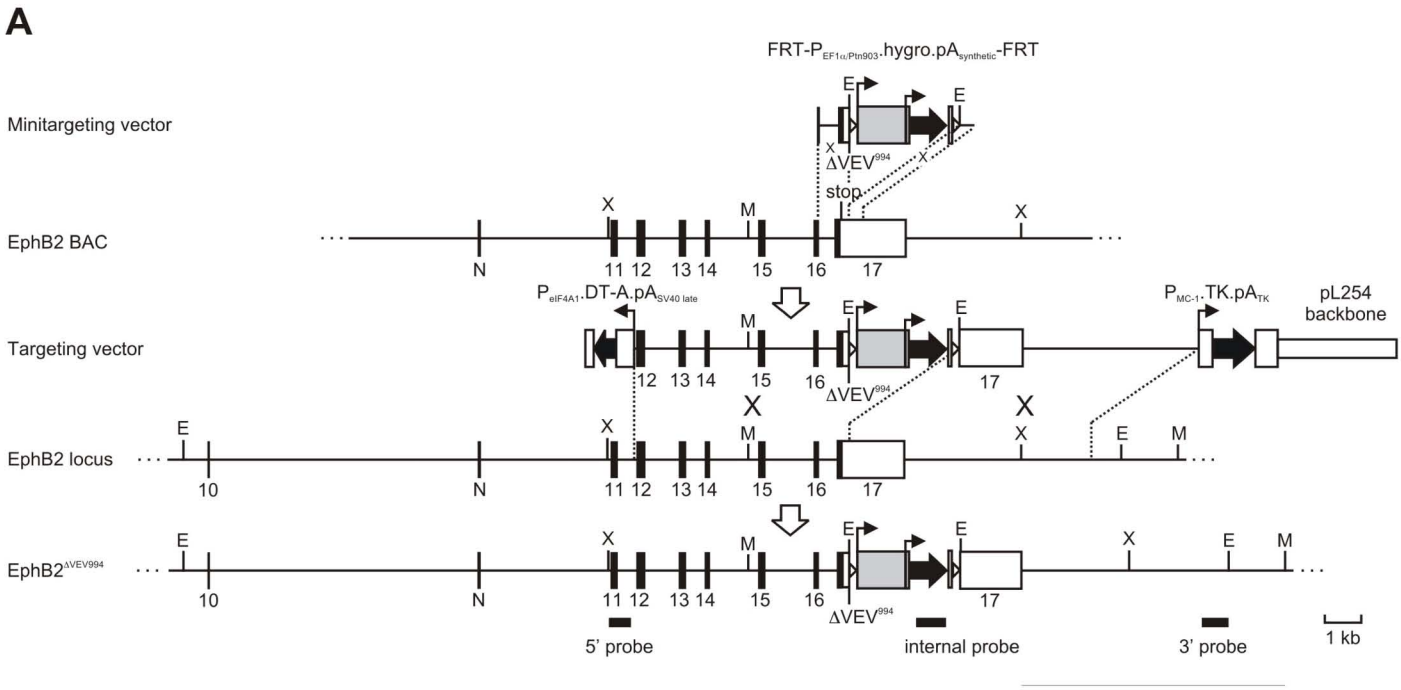
A
FRT-P$_{EF1\alpha/Ptn903}$.hygro.pA$_{synthetic}$-FRT
Minitargeting vector
EphB2 BAC
Targeting vector
EphB2 locus
EphB2$^{\Delta VEV994}$
P$_{eIF4A1}$.DT-A.pA$_{SV40\ late}$
P$_{MC-1}$.TK.pA$_{TK}$
pL254 backbone
ΔVEV$^{994}$
stop
5' probe
internal probe
3' probe
1 kb

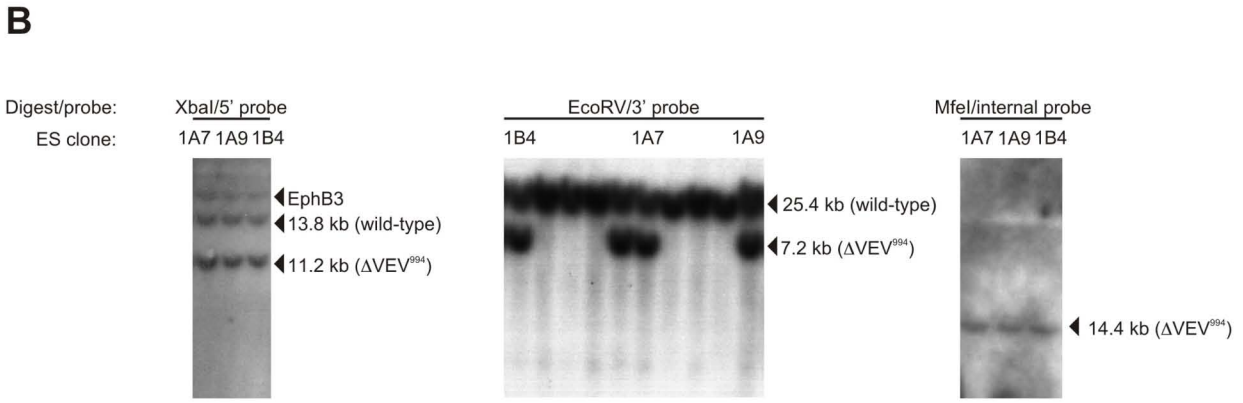
B
Digest/probe:
ES clone:
XbaI/5' probe
1A7 1A9 1B4
EphB3
13.8 kb (wild-type)
11.2 kb (ΔVEV$^{994}$)
EcoRV/3' probe
1B4 1A7 1A9
25.4 kb (wild-type)
7.2 kb (ΔVEV$^{994}$)
MfeI/internal probe
1A7 1A9 1B4
14.4 kb (ΔVEV$^{994}$)

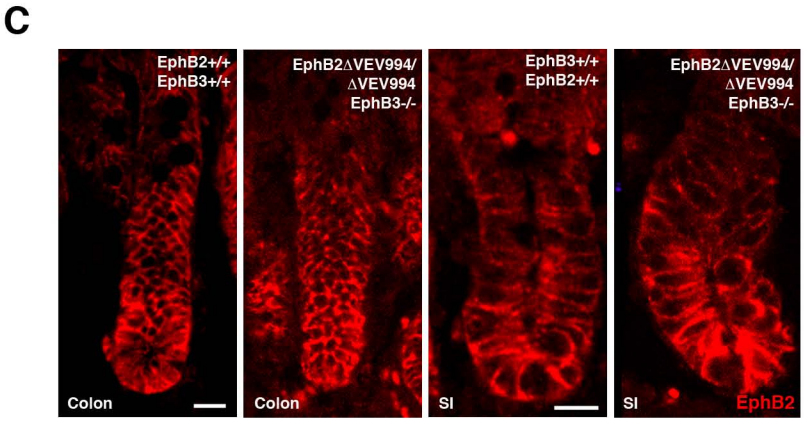
C
EphB2+/+
EphB3+/+
EphB2ΔVEV994/
ΔVEV994
EphB3-/-
EphB3+/+
EphB2+/+
EphB2ΔVEV994/
ΔVEV994
EphB3-/-
Colon
Colon
SI
SI
EphB2

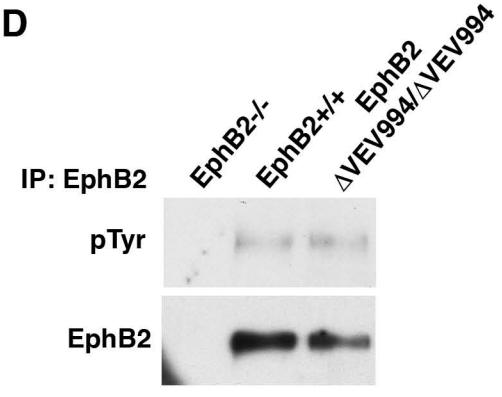
D
EphB2-/-
EphB2+/+
EphB2 ΔVEV994/ΔVEV994
IP: EphB2
pTyr
EphB2

**Figure S1**

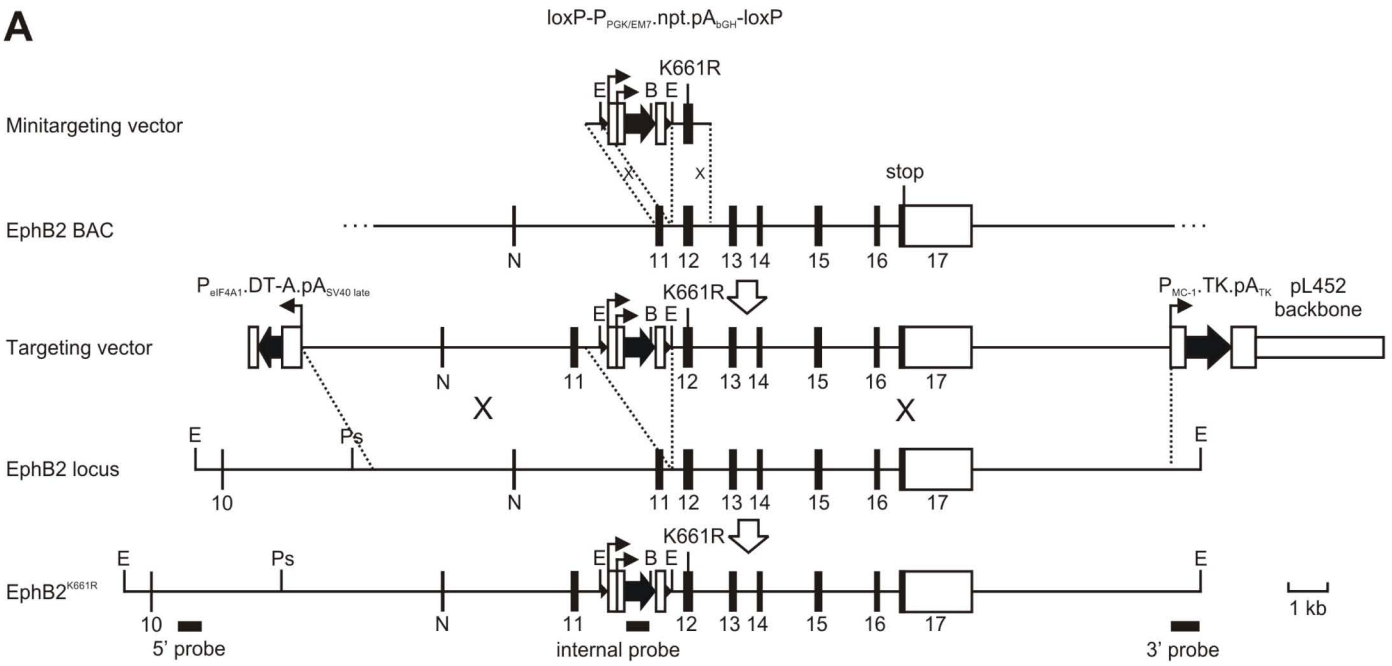
A
loxP-P PGK/EM7 .npt.pA bGH -loxP
K661R
Minitargeting vector
EphB2 BAC
stop
N
11 12 13 14 15 16 17
P eIF4A1 .DT-A.pA SV40 late
Targeting vector
P MC-1 .TK.pA TK
pL452 backbone
EphB2 locus
Ps
10
EphB2 K661R
5' probe
internal probe
3' probe
1 kb

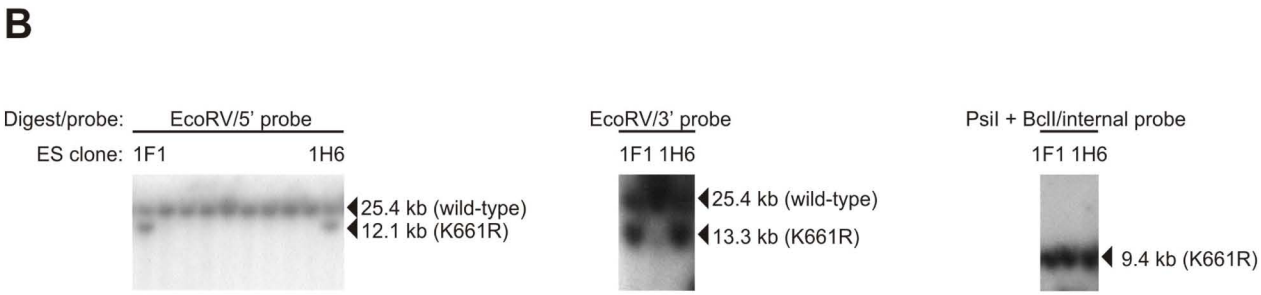
B
Digest/probe:
EcoRV/5' probe
ES clone: 1F1
1H6
25.4 kb (wild-type)
12.1 kb (K661R)
EcoRV/3' probe
1F1 1H6
25.4 kb (wild-type)
13.3 kb (K661R)
PsiI + BclI/internal probe
1F1 1H6
9.4 kb (K661R)

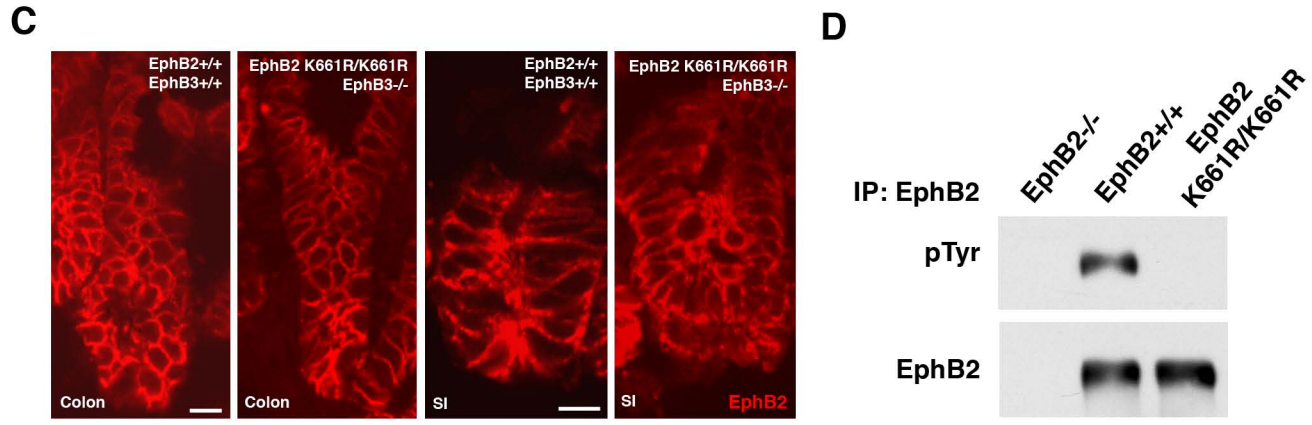
C
EphB2+/+
EphB3+/+
EphB2 K661R/K661R
EphB3-/-
Colon
SI
EphB2
D
IP: EphB2
EphB2-/-
EphB2+/+
EphB2 K661R/K661R
pTyr
EphB2

**Figure S2**

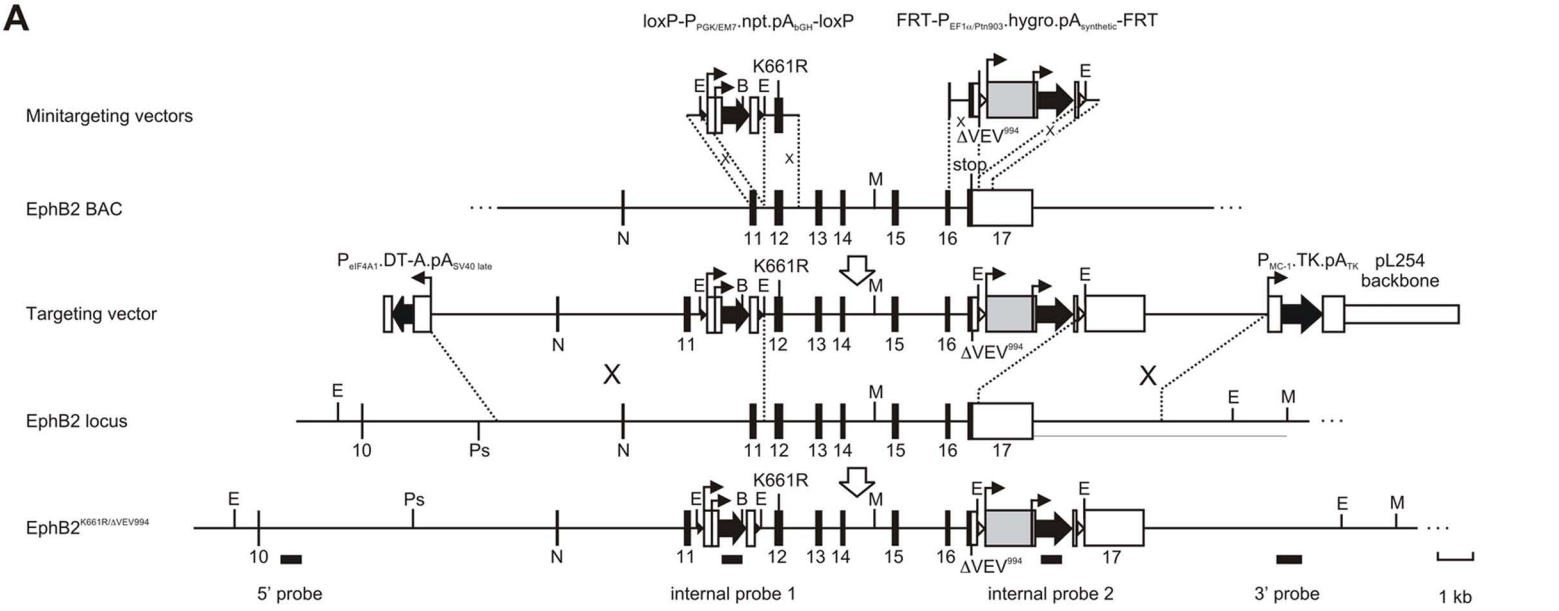
A
loxP-P PGK/EM7 .npt.pA bGH -loxP
FRT-P EF1α/Ptn903 .hygro.pA synthetic -FRT
Minitargeting vectors
EphB2 BAC
Targeting vector
EphB2 locus
EphB2 K661R/ΔVEV994
K661R
ΔVEV994
stop
P eIF4A1 .DT-A.pA SV40 late
P MC-1 .TK.pA TK
pL254 backbone
5' probe
internal probe 1
internal probe 2
3' probe
1 kb

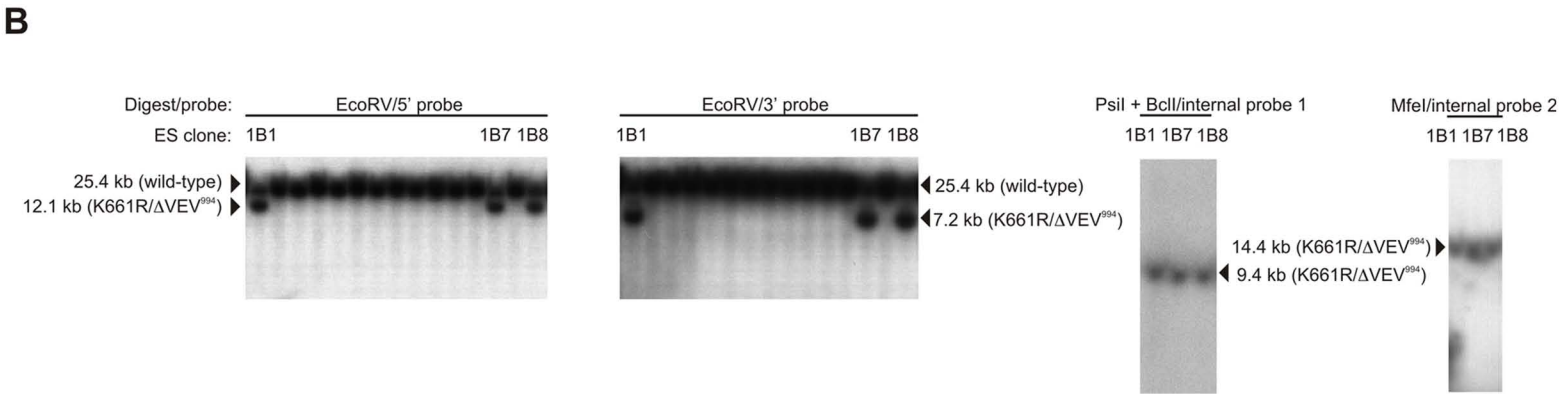
B
Digest/probe:
EcoRV/5' probe
ES clone:
1B1
1B7 1B8
25.4 kb (wild-type)
12.1 kb (K661R/ΔVEV994)
EcoRV/3' probe
7.2 kb (K661R/ΔVEV994)
PsiI + BclI/internal probe 1
MfeI/internal probe 2
14.4 kb (K661R/ΔVEV994)
9.4 kb (K661R/ΔVEV994)

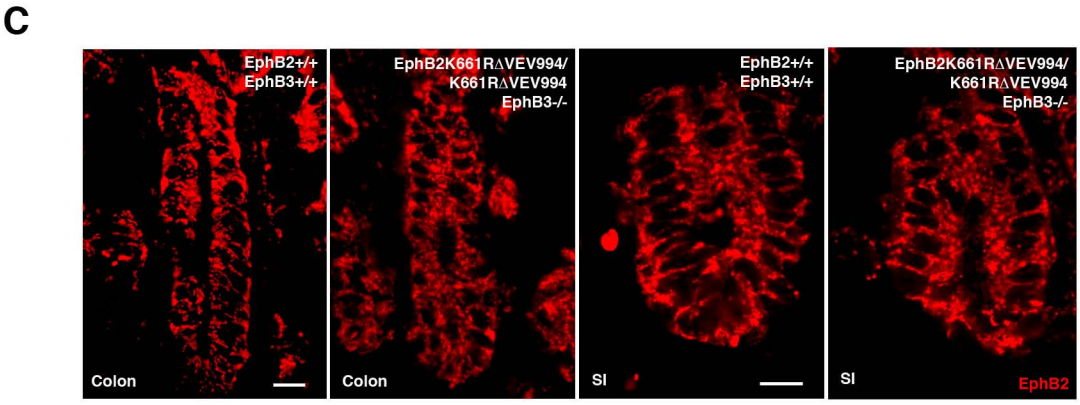
C
EphB2+/+
EphB3+/+
EphB2K661RΔVEV994/
K661RΔVEV994
EphB3-/-
Colon
SI
EphB2

**Figure S3**

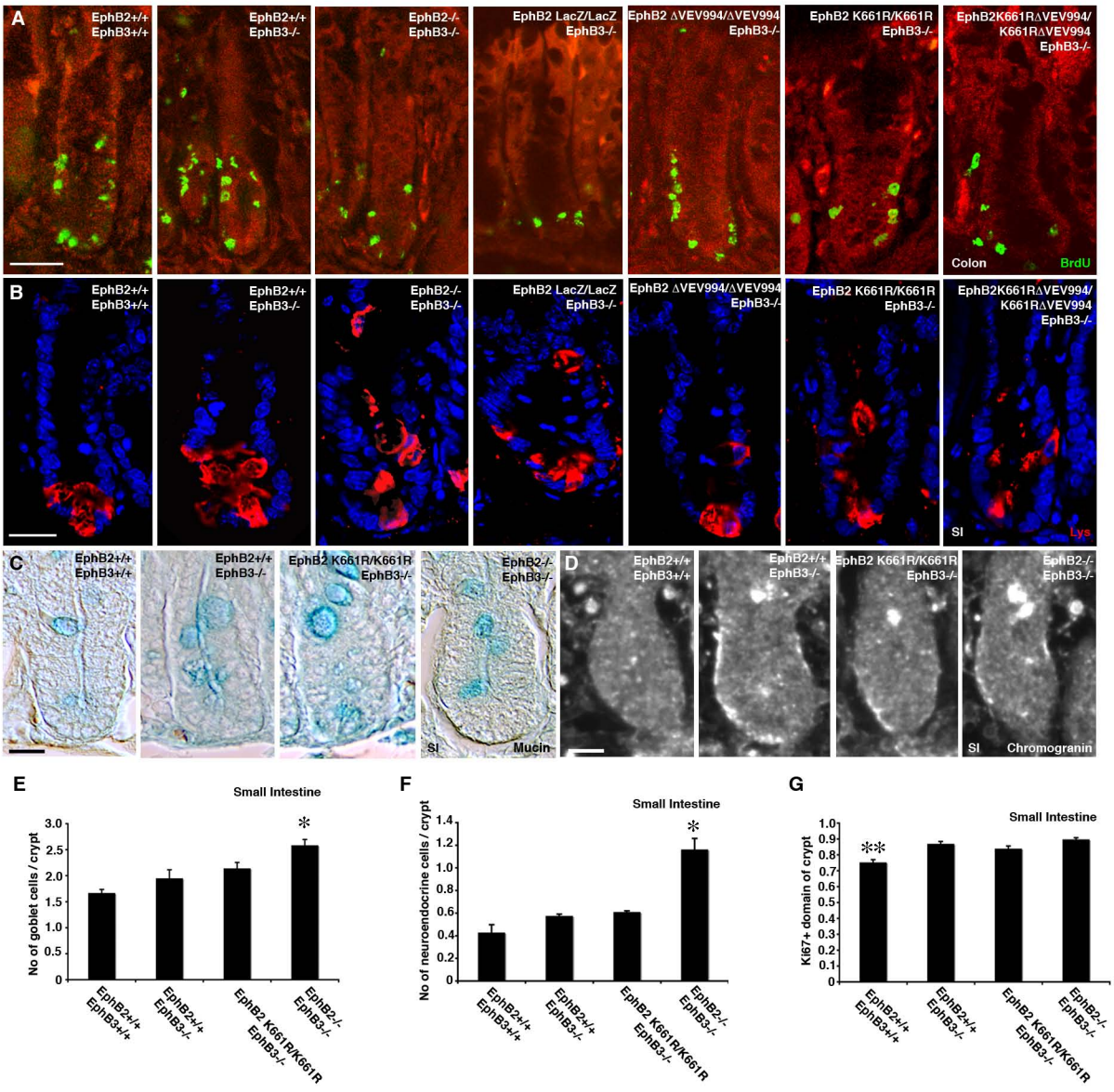
A
EphB2+/+ EphB3+/+
EphB2+/+ EphB3-/-
EphB2-/- EphB3-/-
EphB2 LacZ/LacZ EphB3-/-
EphB2 ΔVEV994/ΔVEV994 EphB3-/-
EphB2 K661R/K661R EphB3-/-
EphB2K661RΔVEV994/ K661RΔVEV994 EphB3-/-
Colon
BrdU
B
SI
Lys
C
Mucin
D
Chromogranin
E
Small Intestine
No of goblet cells / crypt
F
No of neuroendocrine cells / crypt
G
Ki67+ domain of crypt

**Figure S4**

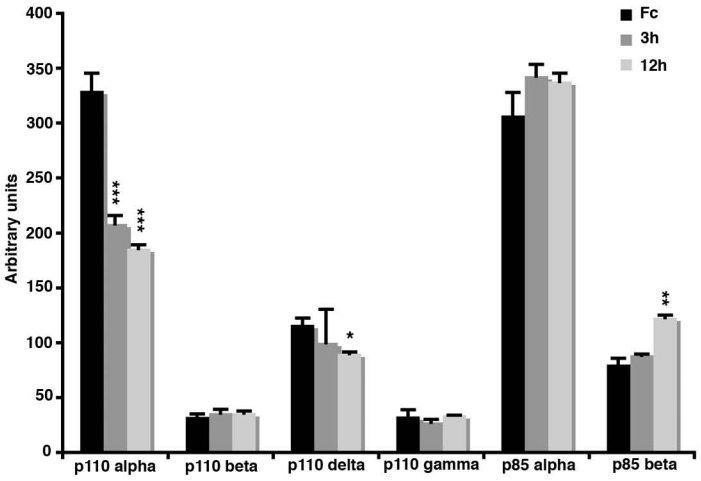
Fc
3h
12h
Arbitrary units
400
350
300
250
200
150
100
50
0
***
***
*
**
p110 alpha
p110 beta
p110 delta
p110 gamma
p85 alpha
p85 beta

Figure S5

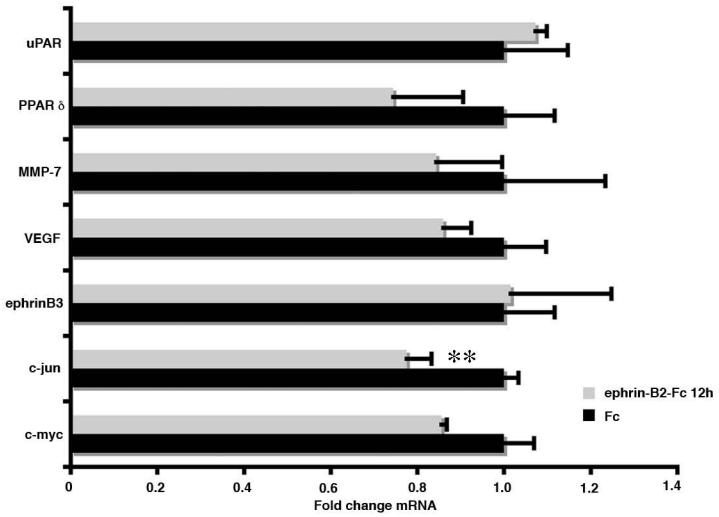
uPAR
PPAR δ
MMP-7
VEGF
ephrinB3
c-jun
c-myc
**
ephrin-B2-Fc 12h
Fc
0
0.2
0.4
0.6
0.8
1.0
1.2
1.4
Fold change mRNA

**Figure S6**

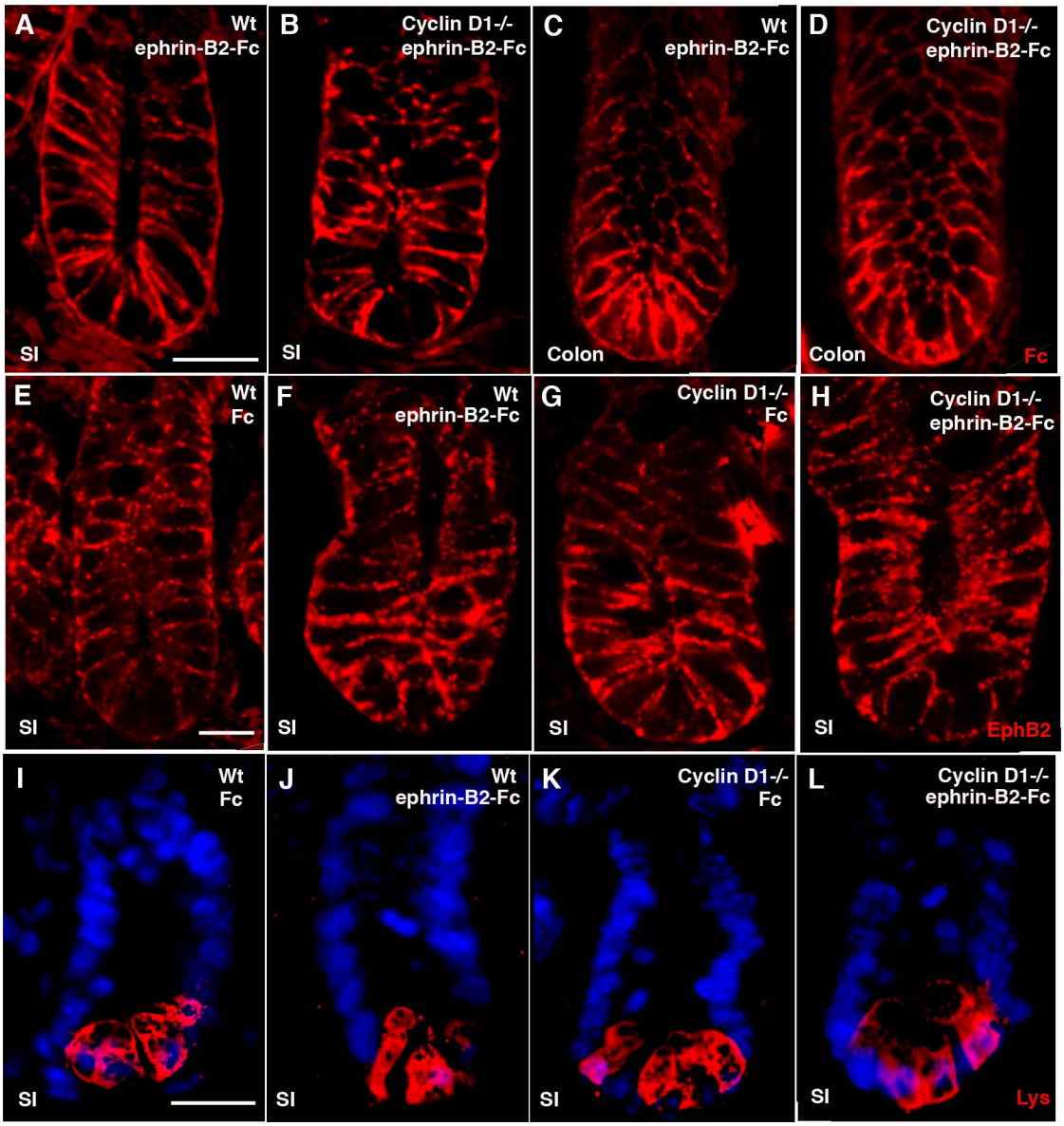
A
Wt
ephrin-B2-Fc
SI
B
Cyclin D1-/-
ephrin-B2-Fc
SI
C
Wt
ephrin-B2-Fc
Colon
D
Cyclin D1-/-
ephrin-B2-Fc
Colon
Fc
E
Wt
Fc
SI
F
Wt
ephrin-B2-Fc
SI
G
Cyclin D1-/-
Fc
SI
H
Cyclin D1-/-
ephrin-B2-Fc
SI
EphB2
I
Wt
Fc
SI
J
Wt
ephrin-B2-Fc
SI
K
Cyclin D1-/-
Fc
SI
L
Cyclin D1-/-
ephrin-B2-Fc
SI
Lys

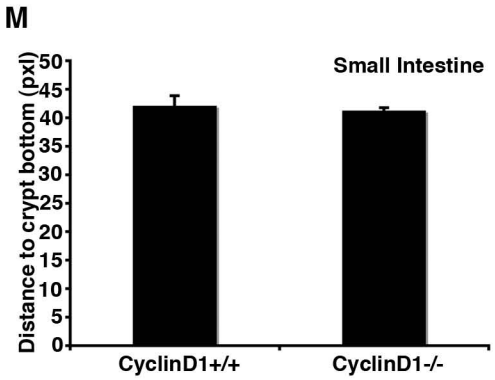
M
Small Intestine
Distance to crypt bottom (pxl)
50
45
40
35
30
25
20
15
10
5
0
CyclinD1+/+
CyclinD1-/-

Figure S7

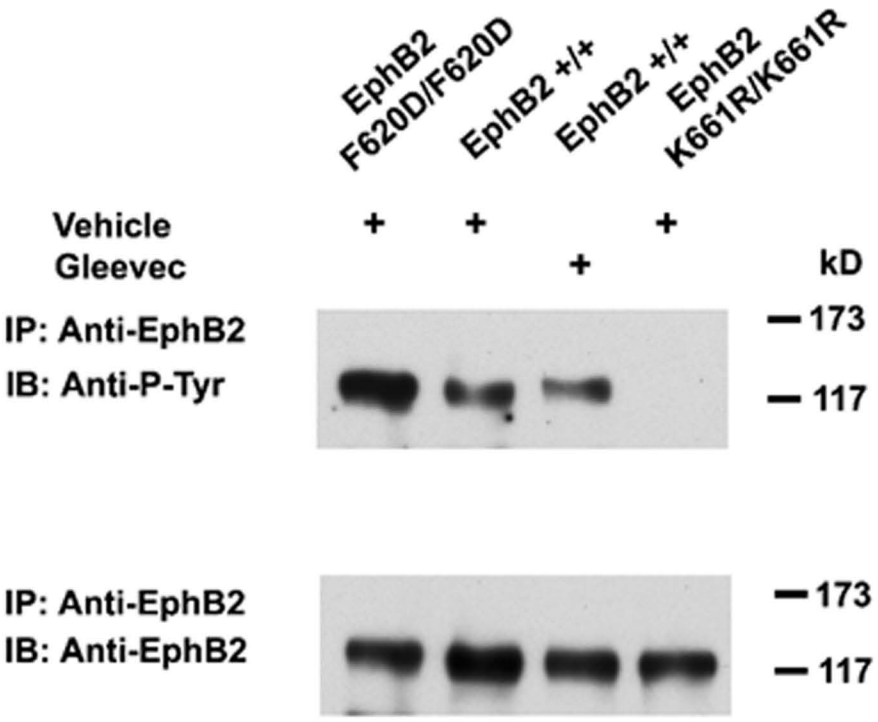
EphB2 F620D/F620D
EphB2 +/+
EphB2 +/+
EphB2 K661R/K661R
Vehicle
Gleevec
+
+
+
+
kD
IP: Anti-EphB2
IB: Anti-P-Tyr
173
117
IP: Anti-EphB2
IB: Anti-EphB2
173
117

**Figure S8**

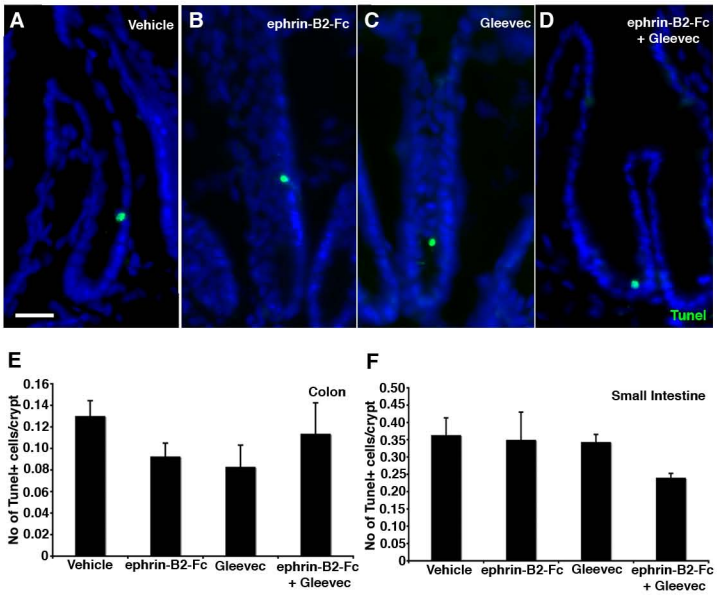
A
Vehicle
B
ephrin-B2-Fc
C
Gleevec
D
ephrin-B2-Fc
+ Gleevec
Tunel
E
Colon
No of Tunel+ cells/crypt
0.16
0.14
0.12
0.10
0.08
0.06
0.04
0.02
0
Vehicle
ephrin-B2-Fc
Gleevec
ephrin-B2-Fc
+ Gleevec
F
Small Intestine
No of Tunel+ cells/crypt
0.50
0.45
0.40
0.35
0.30
0.25
0.20
0.15
0.10
0.05
0
Vehicle
ephrin-B2-Fc
Gleevec
ephrin-B2-Fc
+ Gleevec

**Figure S9**

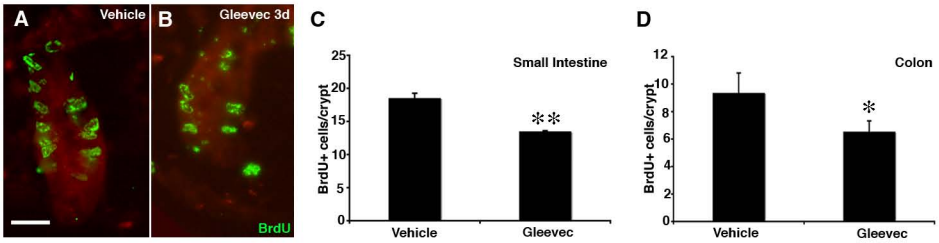
A
Vehicle
B
Gleevec 3d
BrdU
C
Small Intestine
BrdU+ cells/crypt
25
20
15
10
5
0
**
Vehicle
Gleevec
D
Colon
BrdU+ cells/crypt
12
10
8
6
4
2
0
*
Vehicle
Gleevec

**Figure S10**

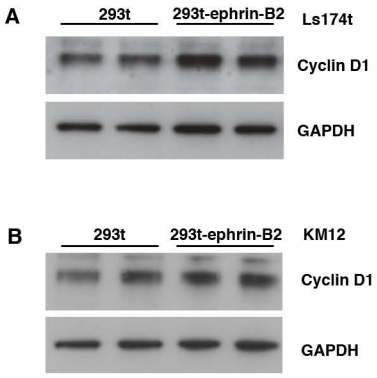
A
293t
293t-ephrin-B2
Ls174t
Cyclin D1
GAPDH
B
293t
293t-ephrin-B2
KM12
Cyclin D1
GAPDH

**Figure S11**

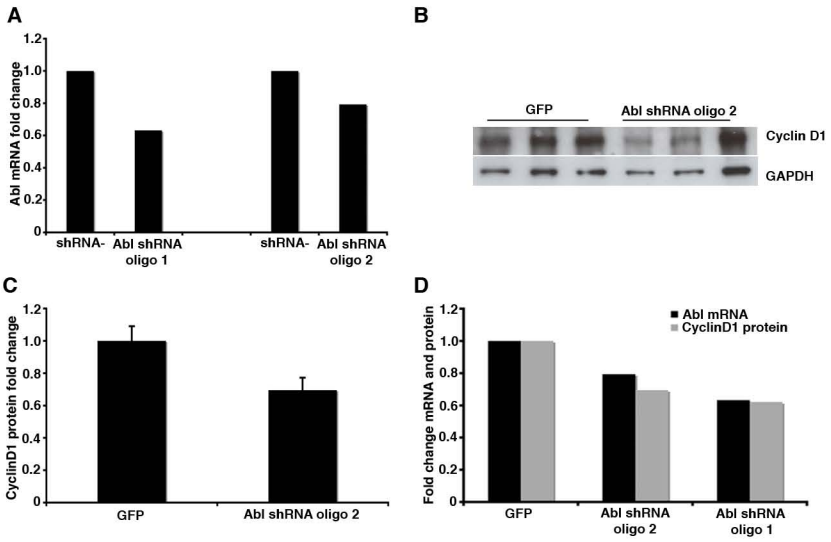
A
Abl mRNA fold change
1.2
1.0
0.8
0.6
0.4
0.2
0
shRNA-
Abl shRNA oligo 1
shRNA-
Abl shRNA oligo 2
B
GFP
Abl shRNA oligo 2
Cyclin D1
GAPDH
C
CyclinD1 protein fold change
GFP
Abl shRNA oligo 2
D
Fold change mRNA and protein
Abl mRNA
CyclinD1 protein
GFP
Abl shRNA oligo 2
Abl shRNA oligo 1

Figure S12

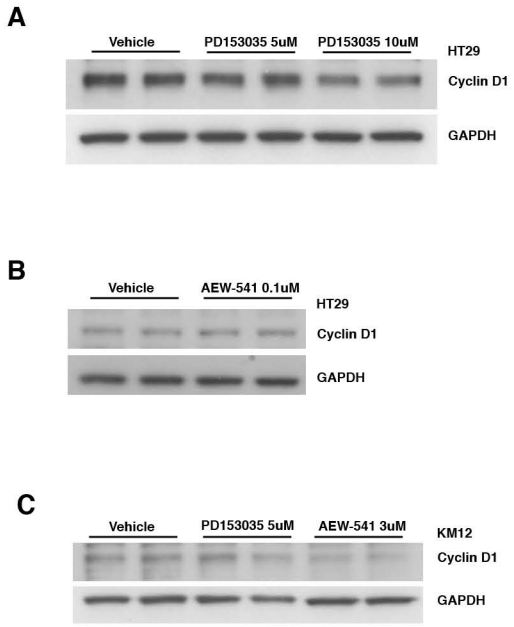
A
Vehicle
PD153035 5uM
PD153035 10uM
HT29
Cyclin D1
GAPDH
B
Vehicle
AEW-541 0.1uM
HT29
Cyclin D1
GAPDH
C
Vehicle
PD153035 5uM
AEW-541 3uM
KM12
Cyclin D1
GAPDH

**Figure S13**

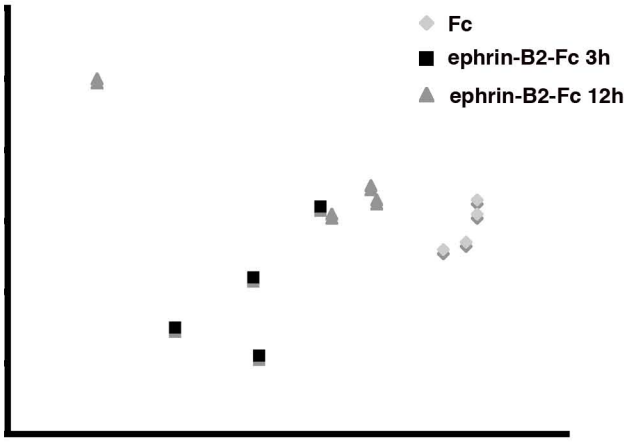


Figure S14

**Ephrin-B2-Fc 12 hours upregulated genes**

| Gene Title | Gene Symbol | p-value |
|---|---|---|
| RIKEN cDNA 1200013P24 gene | 1200013P24Rik | 0.000809 |
| DNA segment, Chr 10, Brigham & Women's Genetics 1364 expressed | D10Bwg1364e | 0.000427 |
| proteasome (prosome, macropain) 26S subunit, non-ATPase, 2 | Psmd2 | 0.000072 |
| triosephosphate isomerase 1 | Tpi1 | 0.000038 |
| FK506 binding protein 5 | Fkbp5 | 0.001363 |
| prohibitin 2 | Phb2 | 0.000316 |
| DnaJ (Hsp40) homolog, subfamily A, member 1 | Dnaja1 | 0.000821 |
| FK506 binding protein 4 | Fkbp4 | 0.000207 |
| DnaJ (Hsp40) homolog, subfamily B, member 1 | Dnajb1 | 0.001154 |
| DnaJ (Hsp40) homolog, subfamily B, member 1 | Dnajb1 | 0.000388 |
| P450 (cytochrome) oxidoreductase | Por | 0.000308 |
| acetyl-Coenzyme A acyltransferase 1A | Acaa1a /// Acaa1b | 0.000389 |
| acetyl-Coenzyme A acyltransferase 1A | Acaa1a /// Acaa1b | 0.001535 |
| solute carrier family 25, member 10 | Slc25a10 | 0.000485 |
| methyltransferase like 7B | Mettl7b | 0.002098 |
| ubiquitin specific peptidase 2 | Usp2 | 0.000001 |
| ubiquitin specific peptidase 2 | Usp2 | 0.000049 |
| huntingtin interacting protein 2 | Hip2 | 0.003301 |
| RIKEN cDNA 9530058B02 gene | 9530058B02Rik | 0.000579 |
| zyxin | Zyx | 0.008163 |
| sphingomyelin phosphodiesterase, acid-like 3B | Smpdl3b | 0.000846 |
| pyruvate kinase, muscle | Pkm2 | 0.000716 |
| tubulin, alpha 4 | Tuba4 | 0.003013 |
| guanine nucleotide binding protein, beta 1 | Gnb1 | 0.000189 |
| period homolog 2 (Drosophila) | Per2 | 0.000022 |
| ferritin light chain 1 | Ftl1 | 0.000335 |
| dynein light chain LC8-type 2 | Dynll2 | 0.000147 |
| serum/glucocorticoid regulated kinase 2 | Sgk2 | 0.010375 |
| amino-terminal enhancer of split | Aes | 0.000784 |
| lamin A | Lmna | 0.000512 |
| potassium channel, subfamily K, member 5 | Kcnk5 | 0.000681 |
| matrix metallopeptidase 15 | Mmp15 | 0.000003 |
| diacylglycerol O-acyltransferase 2 | Dgat2 | 0.000493 |
| ADP-ribosylation factor 5 | Arf5 | 0.000132 |
| heat shock protein 110 | Hsp110 | 0.002633 |
| acyl-CoA synthetase long-chain family member 1 | Acsl1 | 0.000019 |
| RAB1B, member RAS oncogene family | Rab1b | 0.006316 |
| aminolevulinic acid synthase 1 | Alas1 | 0.000064 |
| thyrotroph embryonic factor | Tef | 0.000179 |
| meteorin, glial cell differentiation regulator-like | Metrnl | 0.000000 |
| solute carrier family 39 (zinc transporter), member 1 | Slc39a1 | 0.004116 |
| RIKEN cDNA 5133401N09 gene | 5133401N09Rik | 0.000398 |
| degenerative spermatocyte homolog 2 (Drosophila), lipid desaturase | Degs2 | 0.000769 |
| 2'-5' oligoadenylate synthetase 1A | Oas1a | 0.001215 |
| pleckstrin homology domain containing, family G member 6 | Plekhg6 | 0.011017 |
| RAR-related orphan receptor gamma | Rorc | 0.000165 |

| | | |
|---|---|---|
| cryptochrome 2 (photolyase-like) | Cry2 | 0.000454 |
| glutamic pyruvic transaminase 1, soluble | Gpt1 | 0.000436 |
| RIKEN cDNA C230093N12 gene | C230093N12Rik | 0.000123 |
| RIKEN cDNA C230093N12 gene | C230093N12Rik | 0.000046 |
| heat shock protein 1B | Hspa1b | 0.000198 |
| heat shock protein 1B | Hspa1b | 0.000085 |
| integrin beta 4 binding protein | Itgb4bp | 0.000379 |
| carbonyl reductase 3 | Cbr3 | 0.000411 |
| pyridoxal (pyridoxine, vitamin B6) kinase | Pdxk | 0.001056 |
| CDC42 small effector 1 | Cdc42se1 | 0.000030 |
| cysteine conjugate-beta lyase 1 | Ccbl1 | 0.004317 |
| RIKEN cDNA 1500041J02 gene | 1500041J02Rik | 0.008705 |
| RIKEN cDNA 1700012G19 gene | 1700012G19Rik | 0.000482 |
| myosin IA /// similar to Myosin Ia (Brush border myosin I) (MIHC) | Myo1a /// LOC674795 | 0.000399 |
| RIKEN cDNA 2410127E16 gene | 2410127E16Rik | 0.000096 |
| EF hand domain containing 2 | Efhd2 | 0.000440 |
| aldolase 1, A isoform | Aldoa | 0.000203 |
| solute carrier family 16 (monocarboxylic acid transporters), member 5 | Slc16a5 | 0.000544 |
| cell growth regulator with ring finger domain 1 | Cgrrf1 | 0.017690 |
| --- | --- | 0.000779 |
| triosephosphate isomerase 1 | Tpi1 | 0.000181 |
| RIKEN cDNA 9430029L20 gene | 9430029L20Rik | 0.001614 |
| MARCKS-like 1 | Marcksl1 | 0.000682 |
| eukaryotic elongation factor-2 kinase | Eef2k | 0.002785 |
| solute carrier family 9, isoform 3 regulator 1 | Slc9a3r1 | 0.006039 |
| solute carrier family 9, isoform 3 regulator 1 | Slc9a3r1 | 0.001811 |
| DNA segment, Chr 10, Brigham & Women's Genetics 1364 expressed | D10Bwg1364e | 0.003779 |
| homocysteine-inducible, ubiquitin-like domain member 1 | Herpud1 | 0.005374 |
| uncoupling protein 2 (mitochondrial, proton carrier) | Ucp2 | 0.003620 |
| tetraspanin 4 | Tspan4 | 0.001330 |
| microsomal glutathione S-transferase 3 | Mgst3 | 0.000217 |
| uridine phosphorylase 1 | Upp1 | 0.000063 |
| major vault protein | Mvp | 0.000018 |
| proteasome (prosome, macropain) subunit, beta type 10 | Psmb10 | 0.000008 |
| profilin 1 | Pfn1 | 0.000201 |
| ras homolog gene family, member U | Rhou | 0.001255 |
| ras homolog gene family, member U | Rhou | 0.002591 |
| Usher syndrome 1C homolog (human) | Ush1c | 0.000099 |
| guanine nucleotide binding protein, beta 2 | Gnb2 | 0.000037 |
| solute carrier family 9 (sodium/hydrogen exchanger), isoform 3 regulator 1 | Slc9a3r1 | 0.000021 |
| superoxide dismutase 1, soluble | Sod1 | 0.000518 |
| v-Ki-ras2 Kirsten rat sarcoma viral oncogene homolog | Kras | 0.000074 |
| solute carrier family 35, member C1 | Slc35c1 | 0.000059 |
| heat shock protein 1B | Hspa1b | 0.000068 |
| heat shock protein 1A | Hspa1a | 0.000163 |
| solute carrier family 25 (mitochondrial carrier, glutamate), member 22 | Slc25a22 | 0.005301 |
| cysteine conjugate-beta lyase 1 | Ccbl1 | 0.003896 |
| triosephosphate isomerase 1 | Tpi1 | 0.000022 |

| | | |
|---|---|---|
| clathrin, light polypeptide (Lcb) | Cltb | 0.000139 |
| SEC14-like 1 (S. cerevisiae) | Sec14l1 | 0.000106 |
| CD99 antigen | Cd99 | 0.025346 |
| guanine nucleotide binding protein, beta 1 | Gnb1 | 0.000417 |
| basigin | Bsg | 0.000127 |
| uncoupling protein 2 (mitochondrial, proton carrier) | Ucp2 | 0.006664 |
| uncoupling protein 2 (mitochondrial, proton carrier) | Ucp2 | 0.011469 |
| CNDP dipeptidase 2 (metallopeptidase M20 family) | Cndp2 | 0.000755 |
| platelet-activating factor acetylhydrolase, isoform 1b, beta1 subunit | Pafah1b1 | 0.000014 |
| cysteine and histidine-rich domain (CHORD)-containing, zinc-binding 1 | Chordc1 | 0.000490 |
| DNA segment, Chr 15, Wayne State University 75, expressed | D15Wsu75e | 0.001542 |
| clathrin, light polypeptide (Lcb) | Cltb | 0.000150 |

**Ephrin-B2-Fc 12 hours downregulated genes**

| Gene Title | Gene Symbol | p-value |
|---|---|---|
| cyclin B1, related sequence 1 /// cyclin B1 | Ccnb1-rs1 /// Ccnb1 | 0.000063 |
| zinc finger, A20 domain containing 2 | Za20d2 | 0.000046 |
| nucleolar and spindle associated protein 1 | Nusap1 | 0.000298 |
| solute carrier family 34 (sodium phosphate), member 2 | Slc34a2 | 0.000187 |
| tripartite motif protein 2 | Trim2 | 0.001363 |
| cyclin A2 | Ccna2 | 0.000014 |
| interleukin 18 | Il18 | 0.000884 |
| procollagen, type VIII, alpha 1 | Col8a1 | 0.000071 |
| hydroxyacid oxidase (glycolate oxidase) 3 | Hao3 | 0.000019 |
| nuclear protein 1 | Nupr1 | 0.000140 |
| nuclear protein 1 | Nupr1 | 0.000148 |
| Myosin, heavy polypeptide 9, non-muscle | Myh9 | 0.000833 |
| guanine nucleotide binding protein, alpha 14 | Gna14 | 0.000019 |
| retinitis pigmentosa GTPase regulator interacting protein 1 | Rpgrip1 | 0.000143 |
| deafness, autosomal dominant 5 homolog (human) | Dfna5h | 0.000504 |
| MAD2 (mitotic arrest deficient, homolog)-like 1 (yeast) | Mad2l1 | 0.000053 |
| asp (abnormal spindle)-like, microcephaly associated (Drosophila) | Aspm | 0.003183 |
| meningioma expressed antigen 5 (hyaluronidase) | Mgea5 | 0.012490 |
| ATP-binding cassette, sub-family G (WHITE), member 2 | Abcg2 | 0.000353 |
| dystonin | Dst | 0.003922 |
| RIKEN cDNA 1110007F12 gene | 1110007F12Rik | 0.000096 |
| free fatty acid receptor 2 | Ffar2 | 0.000415 |
| free fatty acid receptor 2 | Ffar2 | 0.000036 |
| hyaluronan mediated motility receptor (RHAMM) | Hmmr | 0.000000 |
| cDNA sequence BC003331 | BC003331 | 0.003049 |
| CDC-like kinase 1 | Clk1 | 0.002398 |
| antigen identified by monoclonal antibody Ki 67 | Mki67 /// LOC638774 | 0.000035 |
| nephroblastoma overexpressed gene | Nov | 0.000046 |
| protein-L-isoaspartate (D-aspartate) O-methyltransferase domain 2 | Pcmtd2 | 0.002845 |

| | | |
|---|---|---|
| centromere autoantigen F | Cenpf | 0.000072 |
| RIKEN cDNA 4833442J19 gene | 4833442J19Rik | 0.001344 |
| premature ovarian failure 1B | Pof1b | 0.000039 |
| TPX2, microtubule-associated protein homolog (Xenopus laevis) | Tpx2 | 0.000319 |
| kelch-like 24 (Drosophila) | Klhl24 | 0.000080 |
| RIKEN cDNA 5730507H05 gene | 5730507H05Rik | 0.000153 |
| cell division cycle associated 1 | Cdca1 | 0.000124 |
| cyclin M4 | Cnnm4 | 0.017338 |
| anillin, actin binding protein (scraps homolog, Drosophila) | Anln | 0.000589 |
| meningioma expressed antigen 5 (hyaluronidase) | Mgea5 | 0.010131 |
| small nucleolar RNA, C/D box 22 | Snord22 | 0.000016 |
| small nucleolar RNA, C/D box 22 | Snord22 | 0.003204 |
| hypothetical protein 6430570G24 | 6430570G24 | 0.000526 |
| expressed sequence C79407 | C79407 | 0.000224 |
| centromere protein E | Cenpe | 0.000129 |
| RIKEN cDNA C730049O14 gene | C730049O14Rik | 0.001359 |
| Protein tyrosine phosphatase 4a2 | Ptp4a2 | 0.001717 |
| Transcribed locus | --- | 0.000319 |
| cytoskeleton associated protein 2-like | Ckap2l | 0.001822 |
| barren homolog (Drosophila) | Brrn1 | 0.003723 |
| RIKEN cDNA 1110014K08 gene /// hypothetical protein LOC664786 | 1110014K08Rik | 0.000036 |
| RIKEN cDNA 4930539E08 gene | 4930539E08Rik | 0.000805 |
| similar to histone 2a | MGC73635 | 0.001835 |
| zinc finger protein 207 | Zfp207 | 0.040902 |
| M-phase phosphoprotein 1 | Mphosph1 | 0.000781 |
| Coiled-coil-helix-coiled-coil-helix domain containing 7 | Chchd7 | 0.000136 |
| guanine nucleotide binding protein, alpha 14 | Gna14 | 0.000110 |
| cyclin B1, related sequence 1 /// cyclin B1 | Ccnb1-rs1 /// Ccnb1 | 0.000078 |
| cell division cycle 2 homolog A (S. pombe) | Cdc2a | 0.001113 |
| PDZ binding kinase | Pbk | 0.000566 |
| claudin 8 | Cldn8 | 0.000137 |
| hyaluronan mediated motility receptor (RHAMM) | Hmmr | 0.000230 |
| centromere autoantigen A | Cenpa | 0.000220 |
| cyclin B2 | Ccnb2 | 0.000187 |
| cell division cycle associated 3 | Cdca3 | 0.000410 |
| GTL2, imprinted maternally expressed untranslated mRNA | Gtl2 | 0.000690 |
| GTL2, imprinted maternally expressed untranslated mRNA | Gtl2 /// Lphn1 | 0.000059 |
| ubiquitin-conjugating enzyme E2C | Ube2c | 0.000113 |
| F-box and leucine-rich repeat protein 3 | Fbxl3 | 0.007493 |
| topoisomerase (DNA) II alpha | Top2a | 0.000465 |
| Transcribed locus | --- | 0.000100 |
| procollagen, type VIII, alpha 1 | Col8a1 | 0.000268 |
| kinesin family member 23 | Kif23 | 0.007374 |
| RIKEN cDNA 2310002J21 gene | 2310002J21Rik | 0.000396 |
| taurine upregulated gene 1 | Tug1 | 0.007830 |
| phosphatidylinositol 3-kinase, catalytic, alpha polypeptide | Pik3ca | 0.000399 |
| high mobility group box transcription factor 1 | Hbp1 | 0.000096 |

**Ephrin-B2-Fc 12h**

| Gene Ontology | p-value |
|---|---|
| cellular physiological process | <0.0001 |
| cell cycle | 0.0001 |
| M phase | <0.0001 |
| M phase of mitotic cell cycle | <0.0001 |
| mitosis | <0.0001 |
| mitotic sister chromatid segregation | 0.009 |
| regulation of mitosis | 0.002 |
| mitotic checkpoint | 0.003 |
| mitotic cell cycle | <0.0001 |
| regulation of cell cycle | 0.0006 |
| regulation of progression through cell cycle | 0.0006 |
| cell division | <0.0001 |
| cytokinesis | 0.01 |
| cell organization and biogenesis | 0.0003 |
| regulation of cell shape | 0.006 |
| cellular localization | 0.0004 |
| establishment of cellular localization | 0.0003 |
| intracellular transport | 0.001 |
| cytoskeleton-dependent intracellular transport | 0.0005 |
| microtubule-based movement | 0.0003 |
| axon cargo transport | 0.003 |
| retrograde axon cargo transport | 0.0003 |
| organelle organization and biogenesis | 0.0003 |
| chromosome condensation | 0.005 |
| cytoskeleton organization and biogenesis | <0.0001 |
| microtubule-based process | <0.0001 |
| monosaccharide catabolism | 0.009 |
| hexose catabolism | 0.009 |
| glucose catabolism | 0.009 |
| glycolysis | 0.006 |
| glucose metabolism | 0.005 |
| fatty acid metabolism | 0.007 |
| protein folding | 0.001 |
| posttranslational protein folding | 0.005 |
| chaperone cofactor-dependent protein folding | 0.003 |
| peptidyl-serine modification | 0.001 |
| peptidyl-serine phosphorylation | 0.001 |
| peptidyl-threonine modification | 0.0006 |
| peptidyl-threonine phosphorylation | 0.0006 |
| chromosome segregation | <0.0001 |
| attachment of spindle microtubules to kinetochore | <0.0001 |
| response to abiotic stimulus | 0.003 |
| response to temperature stimulus | 0.0003 |
| response to heat | <0.0001 |
| response to unfolded protein | 0.0001 |
| response to protein stimulus | 0.0001 |

| Adenoma | EphB2 | CyclinD1 | |
|---|---|---|---|
| P1T1 | 1.013 | 0.988 | |
| P1T2 | 2.030 | 1.372 | |
| P2T1 | 2.316 | 1.029 | |
| P2T2 | 1.382 | 1.175 | |
| P3T1 | 1.036 | 1.103 | |
| 5040 | 1.665 | 1.586 | |
| 6820 | 2.053 | 1.675 | |
| 5004 | 9.179 | 4.319 | |
| 5007 | 11.625 | 1.226 | |
| 8147 | 0.695 | 0.675 | |
| | 3.299 | 1.515 | average |
| | 3.822 | 1.028 | stdev |
| | 1.209 | 0.325 | sem |

| UICC 1 | EphB2 | CyclinD1 | |
|---|---|---|---|
| 5041 | 0.612 | 1.596 | |
| 5055 | 1.133 | 3.062 | |
| 5065 | 1.521 | 0.786 | |
| 5017 | 0.951 | 0.881 | |
| 5048 | 0.714 | 3.159 | |
| 5050 | 0.850 | 0.415 | |
| | 0.964 | 1.650 | average |
| | 0.328 | 1.194 | stdev |
| | 0.134 | 0.488 | sem |

| UICC 2 | EphB2 | CyclinD1 | |
|---|---|---|---|
| 5042 | 1.295 | 0.257 | |
| 5069 | 3.379 | 0.384 | |
| 5078 | 0.899 | 1.119 | |
| 7448 | 0.208 | 0.395 | |
| 5014 | 3.093 | 4.977 | |
| 7011 | 0.359 | 7.088 | |
| | 1.539 | 2.370 | average |
| | 1.373 | 2.930 | stdev |
| | 0.561 | 1.196 | sem |

| UICC 3 | EphB2 | CyclinD1 | |
|---|---|---|---|
| 5026 | 1.090 | 1.191 | |
| 5044 | 1.224 | 1.333 | |
| 5064 | 0.796 | 1.085 | |
| 5052 | 0.312 | 0.466 | |
| 5013 | 1.563 | 3.891 | |
| | 0.997 | 1.593 | average |
| | 0.472 | 1.326 | stdev |
| | 0.211 | 0.593 | sem |

| UICC 4 | EphB2 | CyclinD1 | |
|---|---|---|---|
| 4464 | 1.498 | 1.144 | |
| 5063 | 0.943 | 1.938 | |
| 5693 | 1.532 | 1.556 | |
| 5039 | 1.450 | 1.337 | |
| 5051 | 1.689 | 1.629 | |
| | 1.423 | 1.521 | average |
| | 0.283 | 0.301 | stdev |
| | 0.127 | 0.135 | sem |

Protein levels from human tumor samples
All tumors are normalised against untransformed colon tissue from the same patient

## LEGENDS TO SUPPLEMENTARY FIGURES

**Figure S1 Targeting of the ΔVEV994 mutation to the mouse EphB2 gene**

(A) Exons are numbered and represented by filled boxes (coding) or unfilled boxes (noncoding). Filled arrows represent positive or negative selectable markers, or DT-A. Unfilled arrowheads represent FRT sites. The origin of probes used in Southern blotting analysis and relevant EcoRV (E) and MfeI (M) sites are indicated. P, promoter; $P_{EM7}$, bacterial promoter; PGK, mouse phosphoglycerate kinase; pA, polyadenylation signal; eIF4A1, mouse eukaryotic initiation factor 4A1; hygro, hygromycin phosphotransferase; DT-A, diphtheria toxin-A chain; TK, HSV thymidine kinase; N, novel exon.

(B) Southern blot analysis of three targeted ES cell clones (1A7, 1A9 and 1B4) subsequently used to create chimeric mice.

(C) Immunohistochemical detection of EphB2 demonstrates unaltered distribution in EphB2 ΔVEV994/ΔVEV994; EphB3 -/- mice compared to wild type mice.

(D) EphB2 tyrosine phosphorylation is unaltered in the colon of EphB2 ΔVEV994/ΔVEV994 mice compared to wild type mice. Scale bars=10μm.

**Figure S2 Targeting of the K661R (Codon 661: AAG→AGG) mutation to the mouse EphB2 gene.**

Based on the highly conserved structure of kinase domains, we replaced the essential lysine codon for EphB2 residue 661 situated in the 3rd β-sheet of the N-terminal lobe with arginine (see Figure S2A and S2B for targeting strategy). This lysine residue normally functions to assist in the transfer of ATP to the C-terminal lobe upon receptor activation

through formation of a salt bridge (Wybenga-Groot et al, Cell, 2001, 106: 745-57). Disruption of this salt bridge through the K661R substitution prevents the self-activating phosphorylation of the kinase domain and hence kinase-dependent signaling. (A) Exons are numbered and represented by filled boxes (coding) or unfilled boxes (noncoding). Filled arrows represent positive or negative selectable markers, or DT-A. Filled arrowheads represent loxP sites. The origin of probes used in Southern blot analysis and relevant EcoRV (E), PsiI (Ps) and BclI (B) sites are indicated. P, promoter; PGK, phosphoglycerate kinase; npt, neomycin phosphotransferase; pA, polyadenylation signal; eIF4A1, mouse eukaryotic initiation factor 4A1; DT-A, diphtheria toxin-A chain; PEM7, baterial promoter; TK, HSV thymidine kinase; N, novel exon.

(C) Immunohistochemical detection of EphB2 demonstrates unaltered distribution in EphB2 K661R/K661R; EphB3 -/- mice compared to wild type mice.

(D) EphB2 tyrosine phosphorylation is abolished in the colon of EphB2 K661R/K661R mice. Scale bars=10μm.

**Figure S3 Targeting of the K661R/ΔVEV994 (codon 661: AAG→AGG; Δcodons 992-994) mutations to the mouse EphB2 gene**

(A) Targeting strategy. Exons are numbered and represented by filled boxes (coding) or unfilled boxes (non-coding). Filled arrows represent positive or negative selectable markers, or DT-A. Filled arrowheads represent loxP sites, unfilled arrowheads represent FRT sites. The origin of probes used in Southern blot analysis and relevant EcoRV (E), PsiI (Ps), MfeI (M) and BclI (B) sites are indicated. P, promoter; PGK, phosphoglycerate kinase; $P_{EM7}$, bacterial promoter; npt, neomycin phosphotransferase; hygro, hygromycin

phosphotransferase; pA, polyadenylation signal; eIF4A1, mouse eukaryotic initiation factor 4A1; EF1a, mouse EF1a; DT-A, diphtheria toxin-A chain; TK, HSV thymidine kinase; N, novel exon. (B) Southern blotting analysis of three targeted ES cell clones (1B1, 1B7 and 1B8) subsequently used to create chimeric mice.

(C) Immunohistochemical detection of EphB2 demonstrates unaltered levels and distribution in EphB2 K661R;ΔVEV994/K661R;ΔVEV994; EphB3 -/- mice compared to wild type mice.

Scale bars=10μm.

**Figure S4 Modulation of EphB2 dissociates proliferation from migration**

(A and B) Representative images of BrdU incorporation in colon (A) and distribution of Paneth cells visualized by lysozyme-immunoreactivity in the small intestine (B) of mutant mice. Representative images of mucin positive goblet (C) and neuroendocrine cells (D) distributed in small intestine and the corresponding quantifications (E and F). Measurements of the Ki67 positive domain in small intestine reveals that proliferating progenitor cells are more widely distributed in EphB2+/+:EphB3-/- , EphB2+/+; K661R/K661R and EphB2-/-;EphB3-/- as compared to wild type (G). Scale bar in (A)=20μm and (B) =10μm. Data are represented as mean+SEM.

**Figure S5 Expression of PI3K subunits in the intestine and its regulation by EphB signaling**

Relative expression of mRNA for PI3K subunits. Data from the microarray analysis described in Figure 1.

**Figure S6 EphB signaling does not affect β-catenin mediated transcription**

Analysis of expression levels for genes identified in colon as being regulated by β-catenin-mediated transcription using qRT-PCR showed that only one gene (c-jun) out of the seven genes analyzed was significantly dysregulated ($p=0.03$, Student's t test) in mice 12 hours after ephrin-B2-Fc injection as compared to animals receiving control protein (Fc). Data are represented as mean+SEM.

**Figure S7 Cell positioning in the intestine in the absence of cyclin D1**

(A-D) The systemically adminstered recombinant ephrin-B2-Fc binds EphB receptors in both colon and small intestine (SI) crypts of wild type as well as cyclin D1 mutant mice in a similar pattern, as visualized by using an anti-Fc antibody.

(E-H) EphB2-immunoreactivity forms a similar gradient pattern in the small intestine of wild type and cyclin D1-/- mice. Injection of ephrin-B2-Fc or control Fc protein does not alter the EphB2 levels or distribution.

(I-L) Lysozyme (Lys)-immunoreactive Paneth cells are situated at the bottom of the crypts in the small intestine in both wild type and cyclin D1 null mice. Paneth cells are still positioned at the crypt bottom in both wild type and cyclin D1 mutant mice 24h after inhibition of EphB signaling by an injection of ephrin-B2-Fc. Cell nuclei are labeled with DAPI and appear blue. (M) Quantification of the distribution of Paneth cells in the small intestine of cyclin D1 null mice does not reveal evidence for cell dislocation as compared to wild type littermates.

Scale bar in (A) and (I)=20μm, in (E)= 10μm. Data are represented as mean+SEM.

**Figure S8 EphB2 phosphorylation is not affected by Gleevec**

Immunoprecipitation of EphB2 from EphB2 F620D/F620D reveals increased levels of phosphorylation, whereas the EphB2 K661R/K661R mutant mice show no detectable phosphorylation in comparison with animals expressing a wild type EphB2 receptor. Administration of Gleevec to EphB2+/+ mice does not affect the level of EphB2 phosphorylation.

**Figure S9 Effect of ephrin-B2-Fc and Gleevec on apoptosis**

(A-D) Labeling of apoptotic cells by TUNEL in animals injected with ephrin-B2-Fc, Gleevec or ephrin-B2-Fc and Gleevec. Cell nuclei are labeled with DAPI and appear blue.

(E-F) Quantification of Tunel positive cells revealed no statistically significant difference between animals receiving ephrin-B2-Fc, Gleevec or ephrin-B2-Fc and Gleevec in either colon or small intestine. Data are represented as mean+SEM.

Scale bar=20μm.

**Figure S10 Gleevec inhibits cell proliferation in the intestinal epithelium**

(A-D) Gleevec administration for three consecutive days result in a statistically significant reduction in BrdU incorporation in both the small intestine and colon. Data are represented as mean+SEM. Scale bar=10μm. * = $p \leq 0.05$, ** = $p \leq 0.01$, Student's t test.

**Figure S11 Cyclin D1 regulation in response to ephrin-B2 in transformed human intestinal cells**

(A) EphB expressing Ls174t cells up regulate cyclin D1 when plated together with 293t cells expressing ephrin-B2 but not when plated together with wild type 293t cells. In contrast, plating KM12 cells, a colon carcinoma cell line with low EphB expression, with 293t cells expressing ephrin-B2 does not affect the level of cyclin D1 (B).

**Figure S12 shRNA suppression of Abl expression results in reduced cyclin D1 levels**

Two different Abl shRNA probes were used to transfect HT-29 cells. Both give reduced Abl mRNA expression (A) and cyclin D1 protein levels (B-D, see also Figure 7). The degree of reduction of Abl mRNA correlates to the reduction of cyclin D1 protein.

**Figure S13 EGF and IGF receptor signaling can compensate for the loss of EphB receptors in carcinomas**

HT-29 cells treated with the EGFR-inhibitor PD153035 displays reduced levels of cyclin D1 in a dose dependent manner (A), whereas the IGF-R1 inhibitor AEW-541 does not alter cyclin D1 levels (B). In KM12 cells, cyclin D1 levels are reduced as cells are exposed to the IGFR1, but not the EGFR inhibitor (C).

**Figure S14 Clustering analyses of colon samples injected with control Fc protein or ephrin-B2-Fc**

Analysis of control and ephrin-B2-Fc injected colon reveals that the four control (Fc) replicates cluster together in a group distinct from the ephrin-B2-Fc replicates. The two

different time points of ephrin-B2-Fc used for analysis (3h and 12h) also form two separate groups. Based on the clustering results, one replicate was excluded from further analysis (ephrin-B2-Fc 12 hours replicate 1).

## LEGENDS TO SUPPLEMENTARY TABLES

**Table S1 Analysis of differentially expressed genes 12 hours after inhibition of EphB signaling**

Pair-wise analysis of gene expression data comparing animals injected with ephrinB2-Fc or control protein (Fc) (n=4 in each group) reveals mRNAs up- or down regulated 12 hours after injection. The lists contain transcripts that are differentially expressed in all pair wise comparisons, i.e. 16/16. Corresponding p-values are listed.

**Table S2 Gene ontology themes represented in the ephrin-B2-Fc vs control protein comparison**

Analysis of mRNAs differentially expressed 12h after ephrin-B2-Fc injection (Table S1) as restricted to themes that fall into biological function ($p \leq 0.01$). Corresponding p-values are listed.

**Table S3 EphB2 and cyclin D1 expression in human tumor samples**

Quantified levels of EphB2 and cyclin D1 in human tumors after normalization against untransformed tissue from each patient, with corresponding sample number. Average and standard error of the mean is supplied as these values are used for the graph in Figure 7H and the ratio displayed in Figure 7G.

# Supplemental Data

## Generation of mutant mice

A contig was assembled in pBeloBAC11 from previously described genomic mouse DNA EphB2 lambda phage clones 5.2 and 7.2 (Henkemeyer et al., 1996) using homologous recombination in E. coli. EphB2 exon 12 (for K661R EphB2), exon 17 (for PDZ ΔVEV EphB2) or exons 12 and 17 (for K661R PDZ ΔVEV EphB2) was then targeted, again using homologous recombination in E. coli, with a pL452-based minitargeting vector (Liu et al., 2003) containing EphB2 homology arms; a wild-type 400 bp 5'-arm and an 800 bp, codon 661-mutated (AAG→AGG) 3'-arm to yield pBeloBAC11.EphB2$^{K661R}$, a 1000 bp 5'-arm with a deletion of codons 992-994 and a wild-type 400 bp 3'-arm flanking a FRT-$P_{PGK/EM7}$.hygro.pA-FRT cassette to yield pBeloBAC11.EphB2$^{\Delta VEV994}$ and EphB2 homology arms flanking selectable marker expression cassettes to yield pBeloBAC11.EphB2$^{K661R/\Delta VEV994}$. An EphB2 targeting vector was produced by homologous recombination-mediated retrieval of the modification-containing fragment(s) from pBeloBAC11.EphB2 into pL254 (a modified form of pL253 (Liu et al., 2003) with a DT-A expression cassette and unique AscI site for linearization). All sequences and further details of DNA engineering are available upon request. R1 ES cells were electroporated with AscI-linearized targeting vector, subjected to selection with G418 and gancyclovir and then screened by Southern blotting, all as previously described (Ramirez-Solis et al., 1993). The floxed $P_{PGK/EM7}$.npt.pA cassette was deleted in the mouse germline of EphB2$^{K661R}$ mice by crossing to Cre recombinase-expressing KCN males. The FRT-flanked $P_{PGK/EM7}$.hygro.pA cassette was deleted in the

mouse germline of EphB2$^{\Delta VEV994}$ mice by crossing to FLP recombinase-expressing males. In the EphB2$^{K661R/\Delta VEV994}$ mice, the floxed $P_{PGK/EM7}$.npt.pA cassette was deleted in the mouse germline by crossing to Cre recombinase-expressing KCN males, while the FRT-flanked $P_{EF1\alpha/Ptn903}$.hygro.pA cassette was deleted in the germline of Flp recombinase-expressing males. Genotyping was performed using a two-allele three-primer touchdown PCR. For the EphB2 K661R mice, the oligonucleotides neoF2, (5'-TTGGCTACC CGTGATATTGCTGAA-3'); K661RgF1, (5'-GGGGCCCTACTAAAACCATCAC-3'); K661RgR1, (5'-TTCCTGTCCCATCATTCCCATTG-3') were used. Products were diagnostic of wild-type (300 bp) K661R (671 bp) and K661R$^{\Delta neo}$ (432 bp) alleles. For the EphB2ΔVEV994 mice the oligonucleotides PEF1gR1 : (5'-GCAGCTAATCCCCGCCG ACGAC-3'), dVEVgF1 (5'-GGGGCGGGACAGGCAAGAGA-3') and dVEVgR1 (5'-CCGGTGGCAGCTGGAATGGAC-3'). Products were diagnostic of wild-type (342 bp), ΔVEV994 (598 bp) and Δhygro (491 bp) alleles. All primers were combined in order to genotype the EphB2 K661R/ΔVEV994 mice.

**TOPGAL mouse analysis**

Tissue was fixed in 0.2% glutaraldehyde in PBS at 4º C, permeabilized in 2xpermeabilization buffer (4mM $MgCl_2$, 0.02% NaDOX, 0.04% NP40), after which β-galactosidase was detected using X-gal at a final concentration of 1mg/ml for up to 72 hours at room temperature (He et al., 2007). The tissue was then paraffin sectioned and counterstained. The number of β-galactosidase positive cells in the small intestine was quantified using light microscopy.

**Administration of compounds to mice**

Adult male C57/Bl6 mice were used for all injection experiments. The mice received either 100 µg of ephrin-B2-Fc in PBS (repeated at day 3 for animals analyzed at day 7), administered through the tail vein, or intraperitoneal injection of Gleevec (Imatinib mesylate, Novartis, Switzerland) at a concentration of 100 mg/kg. Gleevec was administered every $12^{th}$ hour to animals sacrificed after 24 hours and once a day to animals sacrificed after 72 hours. LY294002 was administered intraperitoneally once daily for either three or seven days at a concentration of 30 mg/kg. Two hours before sacrifice, animals received BrdU (100mg/kg 0.09% NaCl in PBS), after which they were transcardially perfused with 4% formaldehyde in PBS. Tissues were dissected out and postfixed over night in 4% formaldehyde before being cryoprotected in 20% sucrose in PBS and sectioned at 12 µm on a cryostat.

**Microarray analysis**

Animals were injected with either control protein (Fc) or ephrin-B2-Fc (100 µg/animal) and sacrificed 3 or 12 hours after injection (n=4 in each group). The analysis was carried out on whole colon, as the relative proportion of crypt cells to other cells is larger compared to the small intestine. Total RNA was extracted from rinsed colons using Trizol (Invitrogen) according to manufacturers protocol. Affymetrix Gene Chip Mouse Genome 430A 2.0 was used for the hybridization and all data was analyzed using GeneSifter, Panther (Thomas et al., 2003; Thomas et al., 2006) or GOTM software (http://bioinfo.vanderbilt.edu/gotm/). All samples were normalized according to the Affymetrix MAS5 method after which we applied the MultiDimentional Scaling

approach in order to appreciate differences between the samples. The samples clustered into three groups, corresponding to the Fc, ephrin-B2-Fc 3 hours and ephrin-B2-Fc 12 hours respectively (Figure S14). All original data are uploaded using Tab2MAGE submission to ArrayExpress in compliance with MIAME standards.

**Quantitative PCR**

RNA extraction was done using Trizol (Invitrogen) following the manufacturer's protocol. RNA was stored at -80°C and cDNA was stored at -20°C. RNA quality was assessed using NanoDrop (NanoDrop Technologies Inc.): 260/280 = 1.90-2.12, 260/230 = 1.98-2.25. For the reverse transcription reaction, SuperScript III First Strand (18080-051; Invitrogen) was used. mRNA levels were measured by relative quantification using the standard curve method on a 7300 Real Time PCR System from Applied Biosystems. The standard was made from Mouse Reference Total RNA (750600; Stratagene QPCR). Melting point analysis was performed for all genes to verify that only the desired product had been amplified. β2-microglobulin was used as the internal control against which all individual samples were normalized. The mean value for each group was calculated and the experimental group was normalized against the control group.

**Immunohistochemical analysis**

Cryosections were rinsed in PBS, blocked in 5% goat serum in PBS and incubated with primary antibody at 4˚C over night, washed again in PBS and then incubated with a secondary antibody conjugated to a fluorophor (1:1000, Jackson Laboratories) or to biotin (1:250, Jackson Laboratories). Biotinylated secondary antibodies were detected

using the ABC (VectorLab) and TSA-Cy3 (PerkinElmer) system. BrdU detection required 2M HCl treatment at 37˚ C for 30 minutes. Cyclin D1 levels were detected using the Unmasking Solution from Vector Laboratories (H-3300). Apoptotic cells were detected using the Apoptag Plus Peroxidase In Situ Kit (Chemicon), and the number of positive cells was quantified in each crypt. Goblet cells were detected using an Alcian Blue standard histochemical protocol.

**Western blot analysis**

Tissue taken for western blot analysis was put in ice cold lysis buffer (1M Tris pH 8, 5M NaCl, 10% NP-40, 10% SDS, 10% Na desoxycholate in $H_20$), mixed with Complete protease inhibitor cocktail (Roche) and homogenized using a rotor. Lysates were either analyzed directly using NuPage blot system (Invitrogen) or used for immunoprecipitation using anti-EphB2 (0.2ug/100µl lysate) for 4 hours on ice and then pulled down using Protein A/G sepharose (Amersham) for 1.5 hours on ice. Normalization was performed in two steps. All samples were first normalized to either β -actin or GAPDH, after which the mean value for each group was calculated and the experimental group was normalized against the control group.

**Antibodies**

Antibodies used for immunohistochemistry were rat anti-BrdU (Trichem, Denmark, 1:200), rabbit anti-Ki67 (NeoMarkers, 1:200), goat anti-EphB2 (RnD Systems, 1:500), rabbit anti-Lysozyme (Dako, 1:200) and rabbit anti-cyclin D1 Ab-3 (Neomarkers, 1:100). Antibodies used for Western blot analysis were mouse anti-PCNA Ab-1 (Oncogene, 1:1000), mouse anti-cyclin D1 DCS-6 (NeoMarkers, 1:2000), rabbit anti-cyclin D1

(Abcam ab16663, 1:500), mouse anti-cyclin D2 (Abcam, 1:200), mouse anti-cyclin D3 DCS22 (Cell Signaling, 1:1000), mouse anti-phosphotyrosine clone 4G10 (Upstate, 1:1000), mouse anti-GAPDH (Chemicon, 1:1000), mouse anti- β-actin (Sigma Aldrich, 1:5000), goat anti-EphB2 (RnD Systems, 1:500) and rabbit anti-chromogranin A+B (Progen, 1:50).

**Electroporation**

Small intestine from embryonic day 15 embryos were dissected out and expression plasmids for Abl shRNA and GFP or GFP only (10μg/ul in PBS) was injected into the lumen of a 0.5 cm intestinal segment. The tissue was submerged in PBS and electorporated using 5 pulses (50ms and 60V) using a CUY21 EDIT electroporator (Sonidel). The tissue segments were kept in hanging cultures as described (Hearn et al., 1999) and grown in DMEM:F12 with 10% FBS and 1% penicillin/streptomycin for 15 hours. Before fixation in 4% formaldehyde, BrdU (40ug/mL) was added to the cultures for 1 hour.

**Cell culture**

Non-toxic concentrations for all inhibitors were determined using dilution series. Cells were exposed to BrdU (10 μM) for 30 minutes before they were fixed using 4% formaldehyde or lysed using western blot lysis buffer. Ls174t or KM12 cells were labeled using DiD (V22889 Molecular Probes) and mixed at a 1:1 ratio with either 293t or 293t-ephrin B2-GFP expressing cells and plated in 6-well plate at a density of $5.5x10^5$ cells/$cm^2$. At this density, cells cover the entire plate after attachment, and are forced to

interact with each other. The colon carcinoma cells were FACS purified 18 hours later based on the DiD expression and put in lysis buffer for analysis.

**shRNA transfections**

shRNAs for Abl-1 were purchased from Invitrogen (K4935-00) and sub cloned into a GFP-containing backbone. Constructs were verified by transfecting 3T3 cell lines with Lipofectamine 2000 (11668-027 Invitrogen) according to manufacturer's protocol, after which transfected and non-transfected cells were FACS purified and analyzed using qRT-PCR for Abl RNA expression. Transfection of HT-29 cells was also performed using Lipofectamine 2000 and 24 hours later, cells transfected with either GFP only or Abl shRNA GFP were FACS purified and analyzed using western blot.

***In vitro* cell positioning assay**

293t cells and 293t-ephrin-B2-GFP expressing cells were mixed at a 2:1 ratio and plated in a 24-well plate at a density of $1.3x10^4$ cells/$cm^2$. The cells were cultured for up to 48 hours until they reached confluency. Ls174t colon carcinoma cells were labeled using DiD (V22889 Molecular Probes) according to the manufacturers protocol and then plated on top of the 293t mosaic at a density of 50 000 cells/well. LY294002 (1-5μM) was added to the cultures and the cells were fixed using 4% formaldehyde 18 hours later.

**Quantitative assessment of cell positioning**

Quantification of Paneth cell positioning was done by measuring the distance of each Paneth cell from the crypt bottom. The average distance for each crypt was calculated by

dividing the total distance per crypt with the total number of Paneth cells per crypt. The positioning of neuroendocrine cells and goblet cells was assessed by quantifying the number of respective cell type within the crypt. The length occupied by Ki67+ cells in the crypt was measured to assess the distribution of proliferating progenitor cells.

**References**

He, X.C., Yin, T., Grindley, J.C., Tian, Q., Sato, T., Tao, W.A., Dirisina, R., Porter-Westpfahl, K.S., Hembree, M., Johnson, T.*, et al.* (2007). PTEN-deficient intestinal stem cells initiate intestinal polyposis. Nat Genet *39*, 189-198.

Hearn, C.J., Young, H.M., Ciampoli, D., Lomax, A.E., and Newgreen, D. (1999). Catenary cultures of embryonic gastrointestinal tract support organ morphogenesis, motility, neural crest cell migration, and cell differentiation. Dev Dyn *214*, 239-247.

Henkemeyer, M., Orioli, D., Henderson, J.T., Saxton, T.M., Roder, J., Pawson, T., and Klein, R. (1996). Nuk controls pathfinding of commissural axons in the mammalian central nervous system. Cell *86*, 35-46.

Liu, P., Jenkins, N.A., and Copeland, N.G. (2003). A highly efficient recombineering-based method for generating conditional knockout mutations. Genome Research *13*, 476-484.

Ramirez-Solis, R., Davis, A.C., and Bradley, A. (1993). Gene targeting in embryonic stem cells. Methods in enzymology *225*, 855-878.

Thomas, P.D., Campbell, M.J., Kejariwal, A., Mi, H., Karlak, B., Daverman, R., Diemer, K., Muruganujan, A., and Narechania, A. (2003). PANTHER: a library of protein families and subfamilies indexed by function. Genome research *13*, 2129-2141.

Thomas, P.D., Kejariwal, A., Guo, N., Mi, H., Campbell, M.J., Muruganujan, A., and Lazareva-Ulitsky, B. (2006). Applications for protein sequence-function evolution data: mRNA/protein expression analysis and coding SNP scoring tools. Nucleic acids research *34*, W645-650.